Structure of the γ-tubulin ring complex: a template for microtubule nucleation

Michelle Moritz*†, Michael B. Braunfeld*, Vincent Guénebaut*, John Heuser‡ and David A. Agard*

*Department of Biochemistry and Biophysics, Howard Hughes Medical Institute, University of California, 513 Parnassus Avenue, San Francisco, California 94143, USA

‡Department of Cell Biology, Washington University School of Medicine, 660 South Euclid Avenue, St Louis, Missouri 63110, USA

†e-mail: moritz@msg.ucsf.edu

The γ-tubulin ring complex (γTuRC) is a protein complex of relative molecular mass ~2.2×10^6 that nucleates microtubules at the centrosome. Here we use electron-microscopic tomography and metal shadowing to examine the structure of isolated *Drosophila* γTuRCs and the ends of microtubules nucleated by γTuRCs and by centrosomes. We show that the γTuRC is a lockwasher-like structure made up of repeating subunits, topped asymmetrically with a cap. A similar capped ring is also visible at one end of microtubules grown from isolated γTuRCs and from centrosomes. Antibodies against γ-tubulin label microtubule ends, but not walls, in centrosomes. These data are consistent with a template-mediated mechanism for microtubule nucleation by the γTuRC.

The microtubule cytoskeleton is of fundamental importance to animal cells in interphase for vesicle transport and cell polarity, and to cells in mitosis for formation of the spindle apparatus on which chromosomes separate.

In cells, microtubules are nucleated by the centrosome, which consists of a centriole pair surrounded by a complex set of proteins known as the pericentriolar material (PCM). The PCM contains a fibrous scaffold decorated with hundreds of ring-shaped γ-tubulin-containing structures that are probably sites of microtubule nucleation[1–3]. As PCM is required for microtubule nucleation[4], definition of its structure by high-resolution electron microscopy should shed light on the mechanism by which microtubules are nucleated.

The centrosomal protein γ-tubulin seems to be the key factor in microtubule nucleation (reviewed in refs 5, 6). This protein is known to form complexes within the cell, of which the highly conserved γTuRC is the best characterized so far. This complex contains several copies of γ-tubulin and at least five further proteins, and is thought to be the fundamental unit required for microtubule nucleation (reviewed in refs 6, 7).

When the γTuRC was discovered, two models were proposed to explain how it nucleates microtubules — the so-called 'template' and 'protofilament' models. In the template model, the γTuRC is flush with the minus end of the microtubule, acting as a template; each γTuRC contains 13 γ-tubulin molecules, which interact laterally with one another and each sit at the base of one protofilament[7]. In the protofilament model, γ-tubulin molecules interact longitudinally with one another and the γTuRC unwinds to form the first protofilament of the microtubule, promoting assembly of α/β-tubulin subunits laterally, as well as longitudinally into the microtubule[8]. Here, using electron-microscopic tomography or platinum replicas to investigate the structures of isolated γTuRCs and microtubules nucleated by γTuRCs, and the origins of microtubules within centrosomes, we evaluate the merits of these two models.

Results

Structure of isolated γTuRCs. To study the structure of γTuRCs using electron microscopy, we immunoprecipiated these complexes from early (0–3 h) *Drosophila* embryos (see Methods). Examination of the negatively-stained immunoprecipitate showed that it contained many open-ring-shaped complexes, and separation of the constituent proteins by SDS–polyacrylamide gel electrophoresis (SDS–PAGE) revealed the expected bands (γ-tubulin, Dgrip proteins 163, 128, 91, 84 and 75s; data not shown)[9].

We took two approaches to obtain three-dimensional images of isolated γTuRCs. In the first, we used automated electron-microscopic tomography to obtain many tilted views of negatively-stained γTuRCs, and the resulting data sets were used to reconstruct three-dimensional images of the complexes (see Methods). Four orientations of a representative reconstruction of a γTuRC are shown in Fig. 1a–d. A globular structure sits asymmetrically on one face of the ring (Fig. 1a, c, d); a central slice from the reconstruction shows that this structure is cap-like and probably extends only a limited distance into the ring lumen (Fig. 1b). The ring wall is made up of a series of paired columnar subunits that are distinctly slanted and appear to meet at the capped face of the ring but separate at the other face, giving them an inverted 'U' or 'V' shape (Fig. 1c). We attempted to determine how many of these subunits are present in the ring by examining ~50–100 negatively-stained and cryopreserved γTuRCs (data not shown); the number of subunits varied from 9 to 14, with 12 occurring most frequently. However, given the small sample size, further work is necessary to determine the number of subunits that comprise a functional γTuRC. Almost all complexes studied exhibited a structurally ill-defined gap in the ring, which we presume to be the area where the ring opens, giving it its lockwasher or helical shape. The presence of this region increases the difficulty of counting the subunits.

Our second approach to obtaining three-dimensional images of γTuRCs was to prepare platinum replicas of the complexes using a quick-freeze, deep-etch, rotary shadowing technique[10,11] (see Methods). Samples prepared in this way were similar to those examined by electron-microscopic tomography in that the rings consisted of repeating, columnar subunits (Fig. 1e, upper row and lower-left panel) topped with an asymmetric, globular cap (Fig. 1e, lower row, right two panels). In addition, the helical nature of the complex was strikingly preserved in the platinum replicas (Fig. 1e, upper row). For comparison, we also prepared replicas of pure bovine α/β-tubulin (Fig. 1f). Although articulated rings were found in such samples, their structure is quite distinct from that of the γTuRC.

On the basis of the structures obtained by electron-microscopic tomography and rotary shadowing, as well as on previously published biochemical data on the stoichiometry of the proteins in the γTuRC, which have shown that γ-tubulin, Dgrip84 and Dgrip91 are its most abundant constituents[9], we formulated a proposed structure for the γTuRC (Fig. 1g). The implications of this structure for microtubule nucleation and centrosome attachment are described in the Discussion.

Structure of isolated γTuRCs associated with microtubules. To evaluate the relative merits of the template and protofilament models for microtubule nucleation, we used electron-microscopic tom-

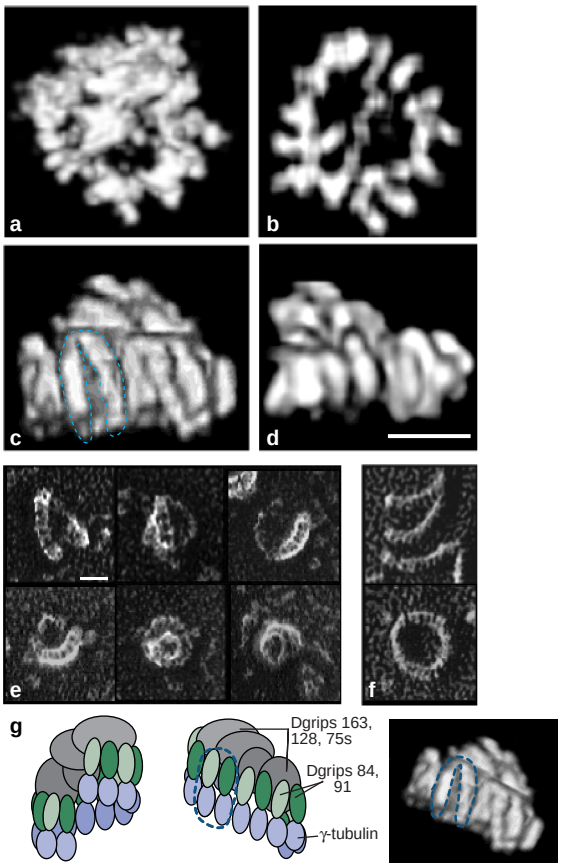

Figure 1 **Structure of isolated γTuRCs. a–d,** Selected views of reconstructed, isolated γTuRCs obtained by electron-microscopic tomography (see Methods). For each image, several sections from the reconstruction were stacked into a single volume and then filtered to enhance contrast and reduce noise. **a**, 'Top' view of the γTuRC, showing the asymmetric 'cap.' The cap sits above the plane of the ring and appears to be mostly contained within the ring lumen. **b**, Middle section of the ring, showing the modular nature of the ring wall as well as a lower remnant of the cap extending from one wall of the ring to the other. This view shows that the bulk of protein in the cap does not extend through the entire ring lumen. **c**, Side view of the γTuRC, showing the repeating columnar subunits that make up the ring wall, topped by the cap. The blue dashed line highlights one V-shaped subunit, which may be one γ-Tubulin small complex (γTuSC, composed of two γ-tubulins, one Dgrip84 and one Dgrip91). **d**, Alternative side view of the γTuRC. The ring-wall subunits and asymmetric cap are apparent. Scale bar represents 10nm. **e,** Platinum replicas of isolated γTuRCs (see Methods). The helical structure and ring-wall subunits are evident in the upper three and lower-left panels. Examples of 'top' views of the asymmetric cap are shown in the right two panels in the lower row (compare to **a**). Scale bar represents 10 nm. **f,** Platinum replicas of pure bovine-brain α/β-tubulin. Tubulin arcs and rings possess subunits, but have distinct structures from those in γTuRCs (compare with **e**). **g,** Model of the γTuRC structure, showing the ring opening (left) and the opposite side (middle). The model incorporates features of the reconstructions and of the platinum replicas — the ends of the ring opening are offset (left), giving it a helical structure. Ring walls are thought to consist of repeating subunits of Dgrip proteins 84 and 91 (green), bound in tandem to γ-tubulin (purple). Dgrip proteins 84 and 91 also interact with each other, particularly at the cap side of the ring, and with the other Dgrip proteins (grey), which may comprise the asymmetric cap. The blue dashed line shows the γTuSC, as in **c**. Right, tilted view of the image in **c**, showing the γTuRC as one might expect it to appear in the absence of helix flattening caused by binding to the grid.

ography to determine the structure of isolated γTuRCs associated with microtubules and the origins of microtubules within the intact *Drosophila* centrosome.

Table 1 End morphologies of microtubules exhibiting named end structures

End structures	Percentage of microtubules exhibiting named end structures	
	+ γTuRCs (n=81)	– γTuRCs (n=87)
Ring/cap + flare	74.1% (60)	4.6% (4)*
Flare + flare	25.9% (21)	94.3% (82)
Ring/cap + ring/cap	0	1.1% (1)*

* These microtubules had one capped end (none had rings).

Microtubules were nucleated on electron-microscopy grids in the presence (+ γTuRCs) or absence (– γTuRCs) of γTuRCs (see Methods). Both ends of microtubules preserved on the grids were examined under the electron microscope to determine the natures of end structures (ring, cap or flare). A total of 81 microtubules was examined on grids containing γTuRCs and 87 microtubules were examined on grids without γTuRCs.

The isolated γTuRC is able to nucleate microtubules *in vitro*[7,9,12]. Therefore, to examine the structure of γTuRCs associated with microtubules, we allowed isolated complexes to adhere to electron-microscope grids which were then incubated with a subcritical concentration of pure α/β-tubulin, allowing microtubules to grow from the immobilized γTuRCs (see Methods). At the α/β-tubulin concentration used (1.5–2.0 mg ml^{-1}), very few microtubules formed on control grids that did not contain γTuRCs (1–3 microtubules per 10 grid squares). However, many microtubules formed on grids containing γTuRCs (~60–100 microtubules per grid square), indicating that the majority of microtubules on the grids may have been nucleated by γTuRCs.

Examination of the morphology of both ends of microtubules on γTuRC-containing grids showed that most (74.1%) had a ring- or cap-shaped closure at one end, as previously observed in γTuRC-nucleated microtubules[7], and a flared opening, characteristic of a growing microtubule[13–17], at the other end (Table 1). In the remaining 25.9%, both ends were flared, indicating either that they were spontaneously nucleated or that they had been released from γTuRCs after nucleation[9]. None of the microtubules examined had rings or caps at both ends. In contrast, 94.3% of microtubules on control grids containing no γTuRCs had flared structures at both ends, a characteristic of spontaneous nucleation, whereas only 4.6% had a cap at one end and a flare at the other, 1.1% had caps at both ends and none had rings.

These microtubule-end-morphology data indicate that most of the microtubules on γTuRC-containing grids may have been nucleated by γTuRCs, and that many may still have been attached to their nucleating complexes. We therefore examined the three-dimensional structures of closed microtubule ends at a higher resolution, using electron-microscopic tomography. Because of the high accelerating voltage (300kV) used, we were unable to determine whether microtubule ends had a ring or a cap structure by simple scanning until after reconstructions were carried out. However, we were able to distuinguish closed and flared ends, and we therefore chose ten microtubules with one closed end and one flared end from which to collect data. Of these, eight had caps at their closed ends and two had rings.

Four representative reconstructions are shown in Fig. 2. The higher resolution provided by electron-microscopic tomography revealed that the cap is asymmetric, with one side concave and the other convex (Fig. 2a–c). This structure is reminiscent of the outline of the ring, with its asymmetric cap, seen in reconstructions of isolated γTuRCs (Fig. 1). In addition, bands of repeating subunits are positioned between the cap and the microtubule (Fig. 2a–c, red arrowheads). These subunits are similar to those observed in the ring walls of isolated γTuRCs (Fig. 1). In two of the reconstructions of γTuRCs bound to microtubules the ring is more prominent than the cap, circling the end of the microtubule; the microtubule appears to grow directly from the ring face (Figs 2d, Fig. 3c).

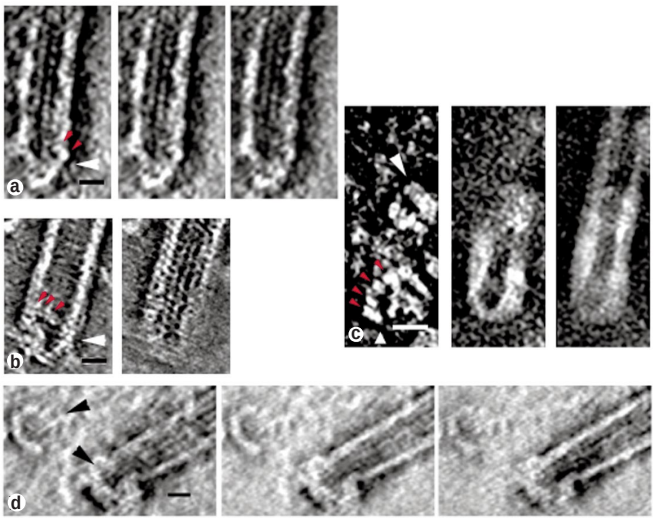

Figure 2 **Reconstructions of isolated γTuRCs in complex with microtubules.** Each set of images represents a sequence of sections moving through the reconstructions. Each panel in each set shows a stack of three to five successive sections. Depending on the reconstruction, each image corresponds to a slice thickness of 1.2 (**a**, **b**), 0.84 (**c**) or 1.69 (**d**) nm. **a–c**, Examples of microtubules with cap-shaped, closed ends. γTuRCs are marked with white arrowheads (a second γTuRC that is not associated with a microtubule is visible in the first panel of **c**. Red arrowheads show bands of subunits that may correspond to modular ring walls (Fig. 1). Note the asymmetry of the closures at microtubule ends, particularly in **a** and **b**; the left side of the structure appears to be concave, the right side convex. **d**, Example of a reconstruction in which the ring structure is more prominent than the cap. Black arrowheads show γTuRCs (the one to the left is not associated with a microtubule). The γTuRC on the right appears to encircle the microtubule origin, with the microtubule growing directly out of one face of the ring; the two ends of the open ring appear to be offset. Scale bars represent 25 nm.

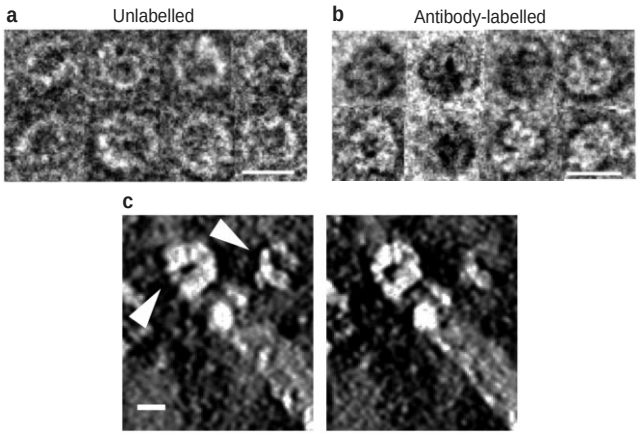

Figure 3. **Comparison of ring-wall widths in γTuRCs labelled with anti-γ-tubulin antibody and in unlabelled γTuRCs. a,** Examples of negatively-stained, unlabelled γTuRCs. Scale bar represents 25 nm. Mean ring-wall width = 7.07 ± 1.67 nm, $n = 39$. **b,** Examples of negatively-stained, antibody-labelled γTuRCs. Scale bar represents 25 nm. Mean ring-wall width = 10.94 ± 1.70 nm, $n = 46$. **c,** Example reconstruction of a microtubule grown from an antibody-labelled γTuRC. The two images represent sequential sections moving through the reconstruction. Each panel shows a stack of three slices. Arrowheads show γTuRCs. Scale bar represents 25 nm.

To confirm that we were observing γTuRCs in these reconstructions and not artefactual structures, we attempted to immunolabel them with gold, using antibodies against γ-tubulin. Unfortunately, the results could not be interpreted because of high background labelling of the grids, which was probably due to the presence of many unoccupied γTuRCs as well as the antigenic γ-tubulin peptide that was used to elute γTuRCs during their isolation. To circumvent this problem, we labelled γTuRCs directly during their isolation using anti-γ-tubulin antibodies coupled to a photocleavable linker. Upon exposure to light, γTuRCs were released with the antibodies still attached (see Methods), and the extra protein (the antibody) associated with the γTuRCs thus increased the dimensions of the ring walls. We measured the widths of the ring walls, comparing antibody-labelled with unlabelled γTuRCs (Fig. 3), and found that labelled ring walls were indeed significantly wider than unlabelled structures (labelled, 10.94 ± 1.70 nm, $n = 46$; unlabelled, 7.07 ± 1.67 nm, $n = 39$; $t(83) = 10.57$, $P < 0.05$, see Methods). A fully extended antibody molecule measures approximately 15 nm, but the observed increase of 0.5 to 7.24 nm in ring wall width is within the expected range, given the lack of information concerning the number of antibodies that bind to γTuRCs and how the antibodies fold onto the rings when bound. The outer diameter of labelled γTuRCs did not increase; instead, the lumen of the ring seemed to be partially filled with antibody, which may account for the increase in ring-wall width. We used labelled γTuRCs to nucleate microtubules on grids and observed rings of the expected larger width at one end of the microtubules (Fig. 3c). The ability of antibody-labelled γTuRCs to nucleate microtubules was identical to that of unlabelled γTuRCs (data not shown). We conclude that the structures we observed in the reconstructions were in fact γTuRCs.

Structure of microtubule origins in centrosomes. In previous electron-microscopic tomography studies we found that we were able to follow individual microtubules through reconstructions back to their origins in isolated *Drosophila* centrosomes. There were no large structures at the ends of the microtubules; they appeared to arise abruptly from the PCM and could be labelled with γ-tubulin antibodies at their sites of contact with the PCM[1,2]. In addition, ring-shaped structures that could be labelled with γ-tubulin antibodies were found in centrosomes without microtubules, indicating that these rings may have been the γTuRCs that had also been isolated from extracts, and that the rings may have acted as templates for microtubule nucleation[1–3]. Because, in this study, we were able to see more detail within isolated γTuRCs and in microtubule-associated complexes, we re-examined the origins of microtubules in centrosomes, this time using higher magnifications and thinner sections (see Methods), allowing us to achieve higher resolution.

We used electron-microscopic tomography to obtain six new reconstructions of unlabelled and anti-γ-tubulin-labelled *Drosophila* centrosomes with regrown microtubule. Two such reconstructions are shown in Fig. 4. The ring structures observed at microtubule bases in unlabelled centrosomes are similar to the structures of isolated γTuRCs (compare Figs 1, 2, 4a, b). Subunits are visible in the ring walls (Fig. 4a) and, when viewed from the side, the ring appears as a cap at the origin of its microtubule (Fig. 4b). In addition, fibres extend from the cap and may attach the γTuRC to the centrosome (Fig. 4b, arrows, orange highlights). For comparison with the ring in Fig. 4a, a cross-section taken from the middle of the microtubule in Fig. 4b is also shown (Fig. 4c). It is clear that the structure at the microtubule origin (Fig. 4a) is different from the structure seen in the microtubule cross-section (Fig. 4c).

In centrosomes labelled with antibodies against the C-terminal 17 amino acids of γ-tubulin, a region that, because of comparison to α/β-tubulin, is expected to be exposed[18], rings were also visible at microtubule origins (Fig. 4d). However, they appeared less distinct than unlabelled structures, probably because of the protein coating applied to the structure during the blocking step of the antibody-labelling procedure. The close and complicated packing of PCM proteins and microtubules within the centrosome make it difficult to find a large number of structures that are unquestionably micro-

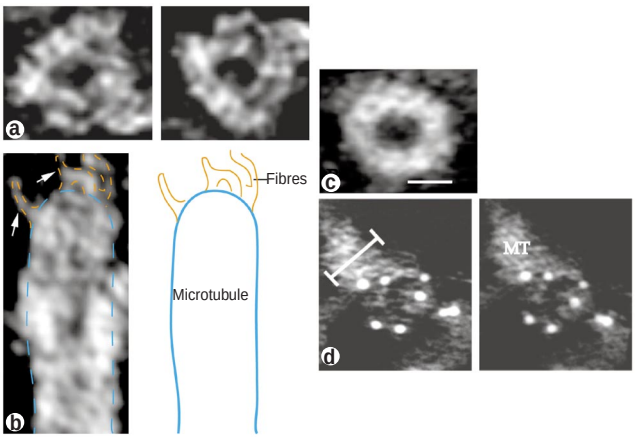

Figure 4. **Reconstructions of microtubule origins in intact centrosomes.** **a–b**, Selected sections of a structure found at the origin of a microtubule. In each panel, several sections from the reconstruction were stacked into a single volume and then filtered to enhance contrast and reduce noise. Note the similarities to the reconstructions of the isolated γTuRC (Fig. 1) and of γTuRCs in complex with microtubules (Fig. 2). Common features of the structures include the modular ring walls (**a**) and the cap structure found at the microtubule origin (**b**). **b**, Left panel, side view of the microtubule that grew from the ring structure shown in **a.** The microtubule, which originates in a cap, is outlined in blue. Arrows and orange outlines show fibres that may connect the γTuRC to the centrosome. Right panel, diagramatic representation of the image in the left panel. **c,** Cross-section of the microtubule polymer. This structure is distinct from that found at the microtubule origin (**a**). Scale bar represents 10 nm. **d,** Part of a reconstruction of an intact centrosome that has been labelled with antibodies against γ-tubulin followed by gold-labelled secondary antibodies. A stereo pair of a labelled microtubule origin within this centrosome is shown; gold particles are arranged in a ring at the microtubule origin. Scale bar represents 25 nm.

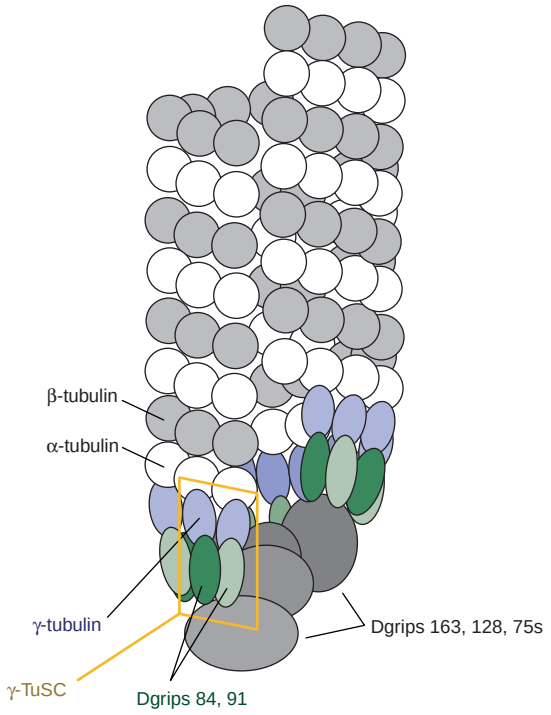

Figure 5. **Model for microtubule nucleation by the 'template' action of the γTuRC.** The ring wall is proposed to consist of six γ-tubulin small complexes (γTuSC; one γTuSC is boxed in yellow), each of which contains two γ-tubulin molecules (purple) and one each of Dgrip84 and Dgrip91 (green). Despite the even number of subunits, the ring is arranged with a 13-fold symmetry. Each of the 12 γ-tubulin molecules is in contact with the minus end of one microtubule protofilament, forming a stable seed that promotes polymerization of the microtubule. Formation of the thirteenth protofilament is promoted by lateral interactions with the twelfth, and possibly the first, protofilaments. The helical nature of the γTuRC imposes the three-start helix on the microtubule. Dgrip proteins 163, 128 and 75s (grey) probably make up the asymmetric cap and maintain the configuration of the ring, and may also form contacts with the centrosome and/or regulate the activity of the γTuRC.

tubule origins. However, in the few cases in which we unambiguously identified gold-labelled microtubule ends, the antibodies were found at the ends of microtubules and did not extend along the sides.

Discussion

The fundamental importance of the microtubule cytoskeleton in eukaryotic cells calls for a detailed, molecular understanding of how microubules are nucleated. A useful approach to solving these mysteries involves high-resolution imaging of the structures involved. We have used electron-microscopic tomography and rotary shadowing to obtain images of the γTuRC in isolation and in association with microtubules, as well as of microtubule origins in centrosomes. These images provide insights into the mechanism of microtubule nucleation by γTuRCs. Our data indicate that this complex may act as a template, as it appears to cap and encircle the end of the microtubule, rather than opening up and extending into the microtubule wall. Given the apparent flexibility of the γTuRC (data not shown[9]), and the fact that microtubules are thought to begin as sheets that close into tubes[13–17], it is possible that the ring is initially open and then closes as the growing microtubule sheet becomes a tube. We found no evidence of this, although immobilization of γTuRCs on grids may have prevented it from occurring. However, we consider this possibility unlikely, given the previous finding that ring-shaped, γ-tubulin-containing structures exist in the centrosome even when microtubules are not present[1–3]. In addition, cryo-electron-microscopy, the electron-microscopic technique that is thought to preserve structures most faithfully[19], also showed γTuRCs in solution to be predominantly ring-shaped (data not shown[9]).

The reconstructions we have obtained lead us to propose models for the arrangement of γTuRC proteins within the complex as well as for points of contact between the γTuRC and the microtubule (Figs 1g, 5). Some of the features of these models have been proposed previously,[5,6,9,20] on the basis of biochemical studies, and it is satisfying that the structural evidence provided by our reconstructions supports them. The repeating subunits in the ring wall are most probably made up of γ-tubulin, Dgrip84 and Dgrip91. The latter two proteins (or their orthologues Spc97 and Spc98 (yeast), and GCP2 and GCP3/HsSpc98p (human)) are known to interact with each other and with γ-tubulin[9,20–22]. In *Drosophila* and *S. cerevisiae*, these proteins have been found to form a small complex that contains two γ-tubulins and one molecule each of Dgrip84 (or Spc97) and Dgrip91 (or Spc98; refs 9, 21, 22). In addition, stoichiometric studies of the *Drosophila* proteins (and some of their *Xenopus* counterparts[6,7]) in the γTuRC show that these three proteins are the most abundant in the complex[6,7,9], indicating that they may comprise the ring wall, where many repeating subunits are visible. Moreover, it is likely that one of the paired, V-shaped subunits corresponds to one γ-tubulin small complex (γTuSC in *Drosophila*[9]; Fig. 1c, blue outline; Fig. 1g; Fig. 5, yellow box). As the height of each column in the subunit (~10 nm) is too great for it to be made up of a single molecule of one of these proteins, we propose a tandem arrangement of Dgrip91 or Dgrip84 with γ-tubulin, as shown in Figs 1g, 5. In this model, the γ-tubulins are located most proximally to the face of the ring that does not contain the cap, and are

therefore available to bind to α/β-tubulin, thereby promoting microtubule growth.

Because of the paired nature of the ring-wall subunits, as well as the independent evidence that there are probably two γ-tubulin molecules in the γTuSC,[9] we propose that there are 12 γ-tubulins in the ring (and therefore 6 γTuSCs), but that a 13-fold symmetry is maintained, probably by the presence of the Dgrip proteins that make up the cap (see below). Each γ-tubulin would thus be in contact with the minus end of one protofilament. The predominance of 13-protofilament microtubules inside cells, as well as in those grown from isolated centrosomes[23,24], can be explained by a model in which formation of the thirteenth protofilament is promoted through lateral interactions with the twelfth, and possibly the first, protofilaments. As factors such as tubulin concentrations, buffer conditions and temperature can influence protofilament numbers *in vitro*[25–27], it is possible that the microenvironment around assembling microtubules inside cells, or even just within the PCM, (involving factors such as tubulin concentration, microtubule-associated proteins and local ion concentrations) may have a bearing on the final protofilament numbers of microtubules. Another possibility is that microtubules inside cells begin with 12 protofilaments and shift to 13 further along the polymer; alteration of microtubule protofilament numbers has been observed in *Xenopus* extracts[27]. Plausible models exist in which the γTuRC contains 14 γ-tubulins (7 γTuSCs) and acts as a template (T. Keating and G. Borisy, unpublished observations this issue.

The platinum replicas of the γTuRC (Fig. 1e) clearly display the helical nature of the complex. It is likely that the offset ends of the ring match the pitch of the 'three-start' helix characteristic of microtubules (reviewed in ref. 28), which would further support the template model. The offset between the ends of the ring may be maintained by one or more of the other complex proteins Dgrip proteins 163, 128 and 75s; ref. 9), which are of lower stoiciometries in the γTuRC[6,7,9], and are therefore assumed, in our model, to make up the cap. These proteins may also be involved in attaching the γTuRC to the centrosome and/or in regulation of the activity of the complex. The fibrous material that extends between the cap and the centrosome (Fig. 4a) supports the idea that the centrosome–γTuRC contact is made here.

The appearance of the cap-shaped structure observed at the minus ends of microtubules (Fig. 2) is very similar to structures observed by Keating and Borisy (this issue) at microtubule ends in *Xenopus* extracts and also in yeast[29–31], at the sites of microtubule attachment to the spindle pole body (SPB). This indicates that the mechanism of microtubule nucleation may be highly conserved and may even extend to yeast, despite the smaller and simpler structure of the γ-tubulin complex in this organism. The fact that the SPB-proximal ends of microtubules in yeast have a very similar appearance to those in flies and frogs indicates that a higher-order structure similar to the γTuRC may be organized by the SPB. This may occur through contacts between the γ-tubulin complex and Spc110p[32,33] or Spc72p[34], proteins at the inner and outer plaques, respectively, that are known to interact with the γ-tubulin complex[21,22].

By obtaining higher resolution images, we will be able to address the remaining structural questions concerning this important protein complex, such as how many subunits the γTuRC actually contains and how each one contacts the protofilaments in the microtubules. It will be interesting to determine whether the isolated γTuRC can dictate the protofilament number or whether further cellular/centrosomal factors are required. Antibody-labelling studies must also be carried out to determine the localizations of individual proteins within the γTuRC. □

Methods

Isolation of γTuRCs and centrosomes.

The procedure for isolation of γTuRCs was as described[9], with the following modifications: NaCl was replaced with KCl in all buffers. The 2% PEG (polyethylene glycol P-2139, mean M_r8,000; Sigma) precipitate of ~30 ml of clarified 0–3 h *Drosophila* embryo extract was resuspended in 12 ml H200 buffer (50 mM K–HEPES pH 7.6, 200 mM KCl, 1 mM $MgCl_2$, 1 mM EGTA, 1 mM β-mercaptoethanol, 0.1 mM GTP, 0.05% IGEPAL CA-630 (Sigma) and 1:1000 protease-inhibitor stock[35]) and clarified by centrifugation for 20 min at 35,000 r.p.m. in an SW55 rotor. 94 μg of an antibody (anti-*Dros*C17) raised against the C-terminal 17 amino acids (QIDYPQWSPAVEASKAG) of the *Drosophila* maternal form of γ-tubulin were added to the clarified supernatant and incubated with gentle rotation at 4 °C for 1 h. The immunoprecipitate was bound to 50 μl Affi-Prep protein A (Bio-Rad) by gentle rotation at 4 °C for 1 h. Beads were then briefly washed with 3×1 ml H200, 3×1 ml H200 minus IGEPAL, and 3×1 ml H100 (50 mM K–HEPES pH 7.6, 100 mM KCl, 1 mM $MgCl_2$, 1 mM EGTA, 1 mM β-mercaptoethanol, 0.1 mM GTP and 1:1000 protease-inhibitor stock), and then eluted by a 9–18-h incubation at 4 °C, without agitation, in 50 μl H100 and 1 mg ml^{-1} C17 peptide.

To isolate γTuRCs labelled with γ-tubulin antibodies, anti-*Dros*C17 antibodies were first coupled to a photocleavable biotin analogue with a long (31.4 Å) spacer arm (EZ-Link; NHS–PC–LC–Biotin, Pierce), according to the manufacturer's instructions. The biotinylated antibodies were then used to isolate γTuRCs from embryo extract as described above, except that the immunoprecipitate was bound to immobilized NeutrAvidin (Pierce), and eluted by ultraviolet irradiation for 15 min to cleave the antibody–linker–Biotin bond, leaving the antibodies bound to the γTuRCs.

Centrosomes were isolated from *Drosophila* embryo extract; microtubules were grown from them as described[35].

γTuRC-mediated microtubule nucleation and electron microscopy.

Grids (50×200 mesh) were coated with formvar, 15 nm gold (for fiducial markers), and carbon. They were then glow-discharged and incubated with 1–3 μl γTuRC for 30 s at 30 °C. The grids were then used to obtain data for reconstructions of γTuRCs alone, or for microtubules grown from immobilized γTuRCs as follows — grid-bound γTuRCs were briefly washed in 80 mM K–PIPES pH 6.8, 1 mM EGTA, 1 mM $MgCl_2$ and 10% glycerol, and then incubated for 5 min with 1.5 or 2 mg ml^{-1} bovine-brain tubulin. Samples were fixed by a 3-min incubation in 1% glutaraldehyde and then washed with distilled H_2O. Samples were briefly stained (<30 s) in 4% uranyl acetate and 1% trehalose, to reduce flattening of microtubules and γTuRCs [36].

Centrosomes with regrown microtubules were labelled with antibodies against γ-tubulin (anti-*Dros*C17, see above) and prepared for electron microscopy as described[1,2], except that 0.25-μm sections (compared with 0.7 μm) of epon-embedded samples were cut and magnifications used for data collections were either ×21,200 or ×30,600 (compared with ×10,000). Tomographic data were collected as follows:

A Philips EM430 electron microscope at 300 kV was used for fully-automated tomographic data collection[37,38]. This instrument is computer-controlled by a Philips C400 interface and a SGI Octane workstation. Data were recorded on a Gatan676-cooled 1,024 × 1,024-pixel slow-scan charge-coupled device (CCD) camera.

For automated tomography, either a room-temperature ultra-high-tilt stage or a high-tilt cryo-holder cooled to –178 °C (both from Gatan) was used. Data were collected at magnifications of either ×30,600 (0.6 or 1.2 nm per pixel, depending on binning) or ×21,200 (0.84 or 1.68 nm per pixel, depending on binning) over angular ranges of ~+70° to –70°, at 1.25°, 1.5° or 2° intervals. Efforts were made to minimize the electron dose during each data collection; total doses were ~1600 electrons $Å^{-2}$.

Processing steps included alignment of the data stack on the basis of colloidal gold markers, conversion of the measured image intensities into a measurement of mass density (mass normalization) and calculation of the reconstruction using resolution-weighted back projection, elliptical-square-weighted back projection or tomographic alternating projection iterative reconstruction. Reconstructions were displayed and modelled using Priism software[38–40]. Six reconstructions of isolated γTuRCs, eleven reconstructions of microtubule-associated γTuRCs and six reconstructions of centrosomes with regrown microtubules (in addition to those published previously[1,2]) were carried out.

Platinum replicas of isolated γTuRCs and of α/β-tubulin were prepared as described[10,11]. Briefly, two drops of a suspension of finely ground mica flakes were added to 0.5 ml of a solution containing isolated γTuRCs or α/β-tubulin, and the protein was allowed to adsorb to the mica for 30 s. Mica flakes were then pelleted by gentle centrifugation, washed twice with a solution of 30 mM Hepes pH 7.2, 70 mM KCl and 5 mM $MgCl_2$, and layered onto a thin slice of aldehyde-fixed lung for support during freezing. This was accomplished by slamming the samples onto the liquid helium-cooled copper block of a homemade quick-freezing device.

Frozen mica flakes were freeze-fractured in a Balzer's freeze-etching unit and etched for 4 min at –100 °C. Molecules absorbed to the mica were rotary-replicated with ~2 nm platinum, applied from an angle of 11° above the horizontal and then backed with a 15-nm film of pure carbon. Replicas were separated from the mica by immersion in concentrated hydrofluoric acid, and then picked up on 75-mesh formvar-coated microscope grids. Replicas were viewed in a JEOL transmission electron microscope at 100 kV; stereo images were obtained using 10° of tilt with a eucentric side-entry goniometer stage.

Measurements of ring-wall widths in antibody-labelled and unlabelled γTuRCs

Unlabeled γTuRCs or complexes labelled with anti-γ-tubulin antibody were applied to electron-microscopy grids and stained with uranyl acetate; their images at ×42,500 were collected using the CCD camera on the EM430 as described above. Using a 'Measure Distances' program within the Priism software[38–40], the widths of 46 labelled and 39 unlabelled γTuRC walls were measured at 6 points around the ring. These six measurements were used to obtain a mean ring width for each γTuRC. The 46 or 39 mean ring widths were, in turn, used to obtain overall mean ring widths for unlabelled and labelled structures. The same approach was used to measure the widths of four labelled and four unlabelled rings observed at the ends of microtubules. In side-by-side comparisons, antibodies associated with γTuRCs did not affect the microtubule-nucleating activity of the complex (data not shown).

RECEIVED 2 FEBRUARY 2000; REVISED 2 MARCH 2000; ACCEPTED 17 APRIL 2000; PUBLISHED 12 MAY 2000.

1. Moritz, M. *et al.* Three-dimensional structural characterization of centrosomes from early *Drosophila* embryos. *J. Cell Biol.* **130,** 1149–1159 (1995).
2. Moritz, M., Braunfeld, M. B., Sedat, J. W., Alberts, B. M. & Agard, D. A. Microtubule nucleation by γ-tubulin-containing rings in the centrosome. *Nature* **378,** 638–640 (1995).
3. Vogel, J. M., Stearns, T., Rieder, C. L. & Palazzo, R. E. Centrosomes isolated from *Spisula solidissima* oocytes contain rings and an unusual stoichiometric ratio of α/β-tubulin. *J. Cell Biol.* **137,** 193–202 (1997).

4. Gould, R. R. & Borisy, G. G. The pericentriolar material in Chinese hamster ovary cells nucleates microtubule formation. *J. Cell. Biol.* **73,** 601–615 (1977).
5. Pereira, G. & Schiebel, E. Centrosome–microtubule nucleation. *J Cell Sci* **110,** 295–300 (1997).
6. Wiese, C. & Zheng, Y. γ-Tubulin complexes and their interaction with microtubule-organizing centers. *Curr. Opin. Struct. Biol.* **9,** 250–259 (1999).
7. Zheng, Y., Wong, M. L., Alberts, B. & Mitchison, T. A γ tubulin ring complex purified from the unfertilized egg of *Xenopus laevis* can nucleate microtubule assembly *in vitro*. *Nature* **378,** 578–583 (1995).
8. Erickson, H. P. & Stoffler, D. Protofilaments and rings, two conformations of the tubulin family conserved from bacterial FtsZ to α-, β- and γ-tubulin. *J. Cell Biol.* **135,** 5–8 (1996).
9. Oegema, K. *et al.* Characterization of two related *Drosophila* γ-tubulin complexes that differ in their ability to nucleate microtubules. *J. Cell Biol.* **144,** 721–733 (1999).
10. Heuser, J. Protocol for 3-D visualization of molecules on mica via the quick-freeze, deep-etch technique. *J. Electron Microsc. Technique* **13,** 244–263 (1989).
11. Heuser, J. Preparing biological samples for stereomicroscopy by the quick-freeze, deep-etch, rotary-replication technique. *Methods Cell Biol.* **22,** 97–122 (1981).
12. Moritz, M., Zheng, Y., Alberts, B. M. & Oegema, K. Recruitment of the γ-tubulin ring complex to *Drosophila* salt-stripped centrosome scaffolds. *J. Cell Biol.* **142,** 775–786 (1998).
13. Erickson, H. P. Microtubule surface lattice and subunit structure and observations on reassembly. *J. Cell Biol.* **60,** 153–167 (1974).
14. Kirschner, M. W., Honig, L. S. & Williams, R. C. Quantitative electron microscopy of microtubule assembly *in vitro*. *J. Mol. Biol.* **99,** 263–276 (1975).
15. Detrich, H. W. D., Jordan, M. A., Wilson, L. & Williams, R. C. Mechanism of microtubule assembly. Changes in polymer structure and organization during assembly of sea urchin egg tubulin. *J. Biol. Chem.* **260,** 9479–9490 (1985).
16. Simon, J. R. & Salmon, E. D. The structure of microtubule ends during the elongation and shortening phases of dynamic instability examined by negative-stain electron microscopy. *J. Cell Sci.* **96,** 571–582 (1990).
17. Chretien, D., Fuller, S. D. & Karsenti, E. Structure of growing microtubule ends: two-dimensional sheets close into tubes at variable rates. *J. Cell Biol.* **129,** 1311–1328 (1995).
18. Nogales, E., Wolf, S. G. & Downing, K. H. Structure of the α/β-tubulin dimer by electron crystallography. *Nature* **391,** 199–203 (1998).
19. Dubochet, J. *et al.* Cryo-electron microscopy of vitrified specimens. *Q. Rev. Biophys.* **21,** 129–228 (1988).
20. Murphy, S. M., Urbani, L. & Stearns, T. The mammalian gamma-tubulin complex contains homologues of the yeast spindle pole body components spc97p and spc98p. *J. Cell Biol.* **141,** 663–674 (1998).
21. Knop, M., Pereira, G., Geissler, S., Grein, K. & Schiebel, E. The spindle pole body component Spc97p interacts with the gamma-tubulin of *Saccharomyces cerevisiae* and functions in microtubule organization and spindle pole body duplication. *EMBO J.* **16,** 1550–1564 (1997).
22. Knop, M. & Schiebel, E. Spc98p and Spc97p of the yeast gamma-tubulin complex mediate binding to the spindle pole body via their interaction with Spc110p. *EMBO J.* **16,** 6985–6995 (1997).
23. Tilney, L.G. *et al.* Microtubules: evidence for 13 protofilaments. *J. Cell Biol.* **59,** 267–275 (1973).
24. Evans, L., Mitchison, T. & Kirschner, M. Influence of the centrosome on the structure of nucleated microtubules. *J. Cell Biol.* **100,** 1185–1191 (1985).
25. Pierson, G. B., Burton, P. R. & Himes, R. H. Alterations in number of protofilaments in microtubules assembled *in vitro*. *J. Cell Biol.* **76,** 223–228 (1978).
26. Böhm, K. J., Vater, W., Fenske, H. & Unger, E. Effect of microtubule-associated proteins on the protofilament number of microtubules assembled *in vitro*. *Biochim. Biophys. Acta* **800,** 119–126 (1984).
27. Chretien, D., Metoz, F., Verde, F., Karsenti, E. & Wade, R. H. Lattice defects in microtubules: protofilament numbers vary within individual microtubules. *J. Cell Biol.* **117,** 1031–1040 (1992).
28. Desai, A. & Mitchison, T. J. Microtubule polymerization dynamics. *Annu. Rev. Cell Dev. Biol.* **13,** 83–117 (1997).
29. Byers, B., Shriver, K. & Goetsch, L. The role of spindle pole bodies and modified microtubule ends in the initiation of microtubule assembly in *Sacchoromyces cerevisiae*. *J. Cell Sci.* **30,** 331–352 (1978).
30. Bullitt, E., Rout, M. P., Kilmartin, J. V. & Akey, C. W. The yeast spindle pole body is assembled around a central crystal of Spc42p. *Cell* **89,** 1077–1086 (1997).
31. O'Toole, E. T., Winey, M. & McIntosh, J. R. High-voltage electron tomography of spindle pole bodies and early mitotic spindles in the yeast *Saccharomyces cerevisiae*. *Mol. Biol. Cell* **10,** 2017–2031 (1999).
32. Kilmartin, J. V. & Goh, P. Spc110p: assembly properties and role in the connection of nuclear microtubules to the yeast spindle pole body. *EMBO J.* **15,** 4592–4602 (1996).
33. Kilmartin, J. V., Dyos, S. L., Kershaw, D. & Finch, J. T. A spacer protein in the *Saccharomyces cerevisiae* spindle pole body whose transcript is cell cycle-regulated. *J. Cell Biol.* **123,** 1175–1184 (1993).
34. Wigge, P. A. *et al.* Analysis of the *Saccharomyces* spindle pole by matrix-assisted laser desorption/ionization (MALDI) mass spectrometry. *J. Cell Biol.* **141,** 967–977 (1998).
35. Moritz, M. & Alberts, B. M. in *Methods in Cell Biology* (ed. Rieder, C.L.) Vol. 61, 1–12 (Academic Press, San Diego, 1999).
36. Harris, J., Gerber, M., Gebauer, W., Wernicke, W. & Markl, J. Negative Stains containing trehalose: application to tubular and filamentous structures. *J. Microsc. Soc. Am.* **2,** 43–52 (1996).
37. Koster, A. J., Chen, H., Sedat, J. W. & Agard, D. A. Automated microscopy for electron tomography. *Ultramicroscopy* **46,** 207–227 (1992).
38. Koster, A. J. *et al.* Towards automatic three-dimensional imaging of large biological structures using intermediate voltage electron microscopy. *Microsc. Soc. Am. Bull.* **23,** 176–188 (1993).
39. Chen, H., Clyborne, W., Sedat, J. W. & Agard, D. A. Prism: an integrated system for display and analysis of three-dimensional microscopy images. *SPIE: Biomedical Image Processing and 3D Microsc.* **1660,** 784–790 (1992).
40. Chen, H., Sedat, J. W. & Agard, D. A. in *Handbook of Biological Confocal Microscopy.* (ed. Pawley, J.) 141–150 (Plenum, New York, 1990).

ACKNOWLEDGEMENTS

We thank C. Wiese and Y. Zheng for help with γTuRC preparations, H. Aldaz for suggesting the EZ-link biotin for antibody labelling, T. Keating for sharing data before publication and for advice on the manuscript, B. Keszthelyi for development of improved image reconstruction approaches, R. McQuity for improved software for automated tomography and T. Mitchison for part of M. M.'s salary. This work was supported by the Howard Hughes Medical Institute and NIH grants GM 31627 (to D.A.A.) and GM23928-22 (to T.M.).

Correspondence and requests for materials should be addressed to M.M.